

# Recent Research Advances in Small-Molecule Pan-PIM Inhibitors

Lei Xu<sup>1</sup> Yu-Cheng Meng<sup>1</sup> Peng Guo<sup>1</sup> Ming Li<sup>1</sup> Lei Shao<sup>2,\*</sup> Jun-Hai Huang<sup>1,\*</sup>

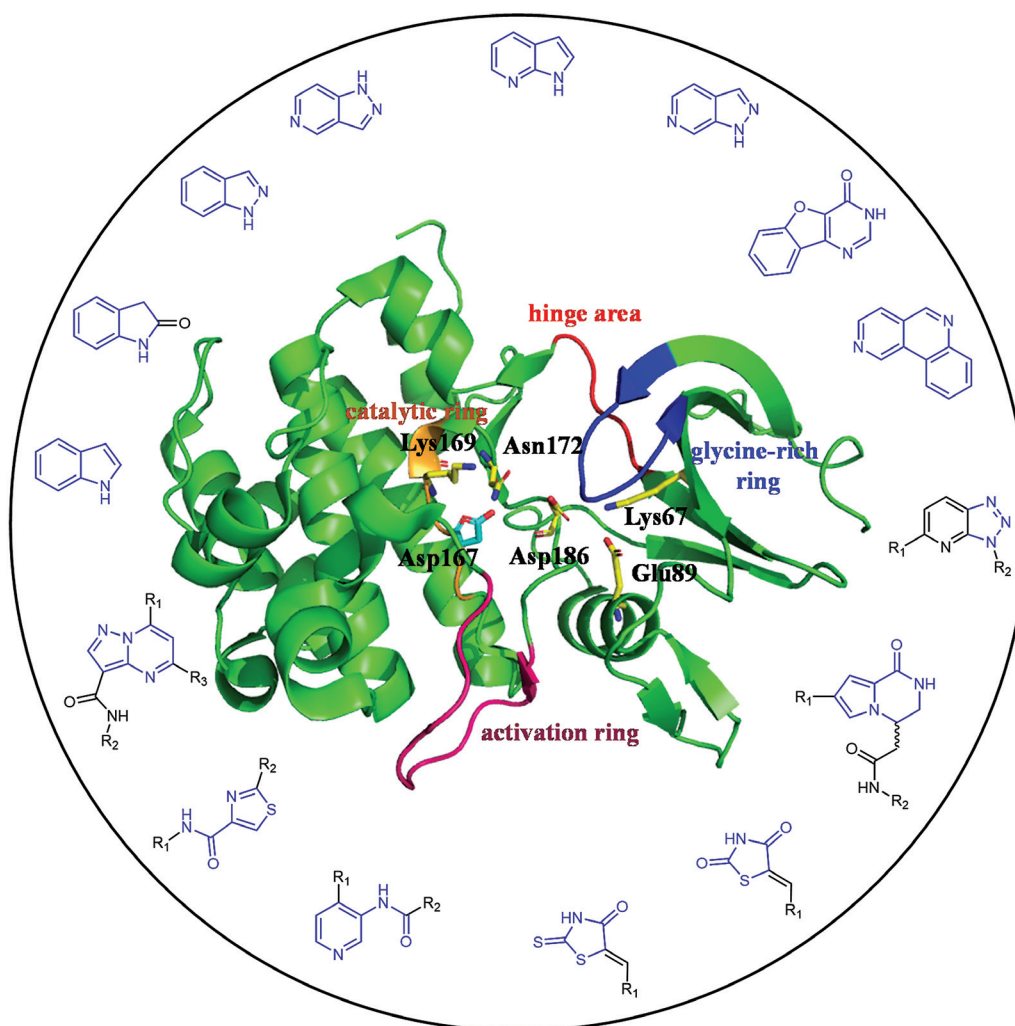
<sup>1</sup> State Key Laboratory of New Drug and Pharmaceutical Process, Shanghai Institute of Pharmaceutical Industry, China State Institute of Pharmaceutical Industry, Shanghai, People's Republic of China

<sup>2</sup> Microbial Pharmacology Laboratory, Shanghai University of Medicine and Health Sciences, Shanghai, People's Republic of China

Pharmaceut Fronts 2022;4:e207–e222.

Address for correspondence Lei Shao, PhD, Microbial Pharmacology Laboratory, Shanghai University of Medicine and Health Sciences, 279 Zhouzhu Road, Pudong New District, Shanghai 201318, People's Republic of China (e-mail: feihusl@163.com).

Jun-Hai Huang, PhD, State Key Laboratory of New Drug and Pharmaceutical Process, Shanghai Institute of Pharmaceutical Industry, 285 Gebaini Road, Pudong New District, Shanghai 201203, People's Republic of China (e-mail: huang\_junhai@163.com).



received  
May 23, 2022  
accepted  
October 14, 2022

DOI <https://doi.org/10.1055/s-0042-1758692>.  
ISSN 2628-5088.

© 2022. The Author(s).  
This is an open access article published by Thieme under the terms of the Creative Commons Attribution License, permitting unrestricted use, distribution, and reproduction so long as the original work is properly cited. (<https://creativecommons.org/licenses/by/4.0/>)  
Georg Thieme Verlag KG, Rüdigerstraße 14, 70469 Stuttgart, Germany

## Abstract

### Keywords

- ▶ pan-PIM inhibitors
- ▶ structure classification
- ▶ lead optimization
- ▶ structure–activity relationship

PIM kinase is consequently emerging as a promising target for cancer therapeutics and immunomodulation. PIM kinases are overexpressed in a variety of hematological malignancies and solid tumors, and their inhibition has become a strong therapeutic interest. Currently, some pan-PIM kinase inhibitors are being developed under different phases of clinical trials. Based on the different scaffold structures, they can be classified into various subclasses. The X-ray structure of the kinase complex outlines the rationale of hit compound confirmation in the early stage. Structure–activity relationships allow us to rationally explore chemical space and further optimize multiple physicochemical and biological properties. This review focuses on the discovery and development of small-molecule pan-PIM kinase inhibitors in the current research, and hopes to provide guidance for future exploration of the inhibitors.

## Introduction

The proviral integration site for moloney murine leukemia virus (PIM) kinase belongs to the serine/threonine kinase family and involves three highly homologous enzymes, including PIM1, PIM2, and PIM3. They have similar functions and kinase domain but differ in their distribution in tissues and organs.<sup>1</sup> PIM1 is mainly expressed in hematopoietic tissues, PIM2 is expressed in lymphoid and brain tissues, while PIM3 is more abundant in the brain, kidneys, and the epithelia.<sup>2,3</sup> PIM kinase is primarily responsible for cell cycle,<sup>4</sup> and its overexpression is often associated with the development of many malignant hematomas and solid tumors.<sup>5–7</sup> Its role in modulating immune microenvironments and regulating immune cells has also been reported.<sup>8</sup> Recently, inhibition of PIM kinases has emerged as a hot spot in drug development, and has been widely used to reduce glycolysis, increase T cell persistence, and control tumor processes.<sup>9–11</sup>

The binding mode between inhibitors and receptors indicated that PIM1 kinase immobilized the molecule in the active center of the enzyme between residues of Lys67, Glu89, Asp186, and the molecules (▶ **Fig. 1**). Besides, PIM kinases have the amino-cyclized Pro123 residue in the hinge region of the ATP-binding pocket and therefore lacks the hydrogen-bond donor property.<sup>12,13</sup> This creates a molecular recognition motif that is unique among the kinase family members. Thus, taking well advantage of these structural features is vital for designing potent pan-PIM inhibitors.

Compared with PIM1 and PIM3, PIM2 has a 10–100-fold lower affinity for ATP, thus, PIM2 is more difficult to target, and the identification of pan-PIM inhibitors has been more challenging. Evidence suggested that knockout of PIM1 gene is associated with the increased expression of PIM2, while knockout of PIM1 and PIM2 at the same time leads to abnormally increased expression of PIM3.<sup>14</sup> Considering these points, pan-PIM inhibition appears to be the most

desirable strategy for the optional efficacy and results in relatively fewer concomitant toxicities. Herein, we present the discovery of potent and selective active inhibitors of all three PIM kinases.

## Structure Classification of Clinical Pan-PIM Kinase Inhibitors

SGI-1776 is a representative of the first generation of PIM inhibitors that are focused on imidazo[1,2-*b*]pyridazine derivatives.<sup>15,16</sup> The drug is a pan-PIM inhibitor with nanomolar activity, and also exhibits inhibition activity against FLT3 kinase, but unfortunately discontinued in phase 1 due to a narrow therapeutic window against cardiotoxic side effects linked to hERG inhibition. ▶ **Table 1** lists several novel competitive pan-PIM inhibitors, including PIM447 (LGH447) and INCB053914, that have been advanced in early clinical trials, providing evidence of developing durable single-agent efficacy in human clinical trials, and further reinforcing the inhibition of PIM kinase as a promising therapeutic strategy for the treatment of diseases.<sup>17–20</sup>

### Benzothienopyrimidinone

Hit **1** was identified by Tao et al with the help of high throughput screening (HTS; ▶ **Fig. 2**).<sup>21</sup> Examination of crystal structures of protein kinases facilitated in-depth study of their unique ATP-binding pockets and provides computational and medicinal chemistry opportunity for a selective inhibition. Tao et al studied a molecular docking of **1** with PIM1 kinase (PDB code: 3JYA), and it revealed that the 2-position of the pyrimidinone ring is exposed to the solvent-accessible region, while the 8-position of phenyl ring is in the hydrophobic area, so some polar and hydrophobic groups can be accommodated in these two positions, separately. Considering the poor kinase selectivity and cellular activity of **1**, phenyl substitution at 8-position was performed. The results showed that phenyl substitution at 8-position could significantly enhance PIM inhibitory activity, with **2** being the most active analogue. Compound **2** showed

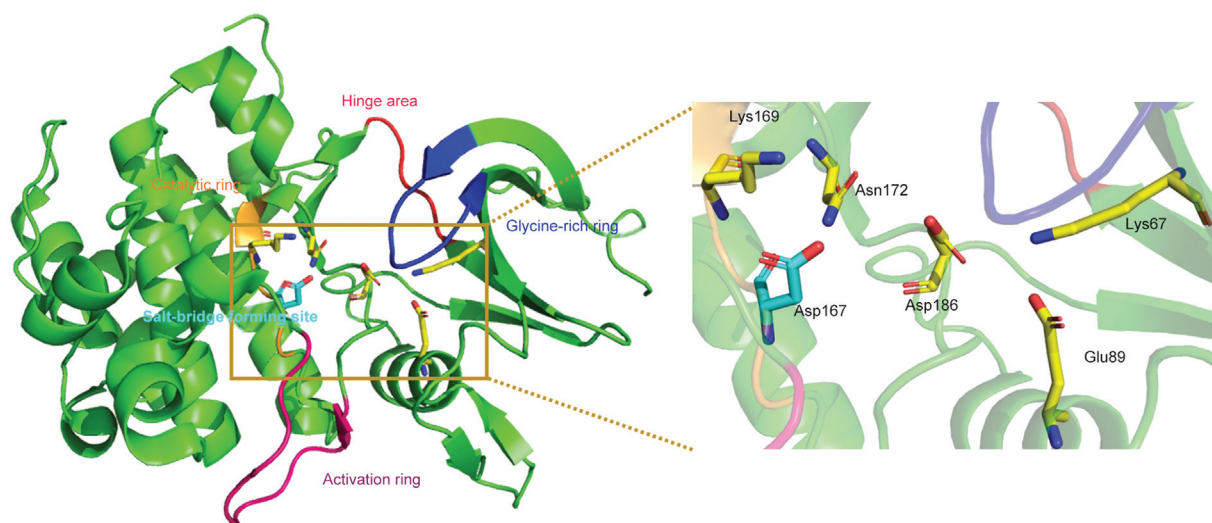


**Fig. 1** PIM1 kinase protein (PDB: 1XQZ). Illustration: the proton acceptor site (Asp167) and the activation domain (Lys67, Glu89, Lys169, Asn172, and Asp186) are highlighted in a close-up view with a stick model. The glycine-rich ring (Leu44-Val52), hinge area (Glu121-Pro125), catalytic ring (Arg166-Asp170), activation ring (Ala191-Asp202), and salt-bridge-forming site (Asp167) are shown in *blue, red, orange, pink, and light blue*, respectively.

a high affinity for three PIM kinases (PIM1, PIM2, and PIM3) with  $K_i$  values of 2, 3, and 0.5 nmol/L, respectively. Moreover, **2** exhibited a good bioavailability of 76% after oral dosing in a CD1 mice model. ADME (absorption, distribution, metabolism, and excretion) profiling of **2** suggested a long half-life in both human and mouse liver microsomes, good permeability, modest protein binding, and no cytochrome inhibition below 20  $\mu$ mol/L. Given above, exploring benzothienopyrimidinone scaffolds for pan-PIM kinase inhibition has shown great potential.

### Benzofuopyrimidinone

Protein kinases CK2 and PIM have structural similarity in their ATP-binding site. They have synergistic roles in oncogenic pathways and exploring dual kinase inhibitors is a reasonable starting point for drug design.<sup>22</sup> In view of the facts mentioned above, Tshuhako et al intend to incorporate a pyrimidinone CK2 inhibitor into benzofuopyrimidinone **3**, a pan-PIM inhibitor with only moderate potency. Then, analog **4** was achieved, which showed improved PIM1 and PIM3 activities with modest selectivity over CK2 (**Fig. 2**).<sup>23</sup> Molecular docking revealed the modes of interaction of **4** with the PIM1 kinase active site (PDB code: 4ALU). The results suggested that 8-Br is necessary for binding activity as it is packed tightly against the hinge region. Right-hand modifications of the aryl ring were performed to design analogs including **5** that interact with Asp128, Asp131, and Glu171 in the ATP pocket via hydrogen bonding. Interestingly, pan-PIM inhibitory potency and selectivity were significantly improved. Then, modifications with alkyl groups on the right hand of the aryl ring suggested that alkyl amino benzofuopyrimidinones were as potent in PIM as the aryl benzofuopyrimidinones, with  $IC_{50}$  values ranging from 4 to 68 nmol/L, and, more importantly, showed enhanced cellular permeability. Among those compounds, **6** is an ideal lead. **6** exhibited high plasma exposures (1 h/4 h) in mouse dosed at 100 mg/kg and associated with a favorable rat pharmacokinetic (PK) profile with high bioavailability and

good absorption. Additionally, **6** could inhibit phosphorylation of BAD at the PIM kinase-specific site Ser112 in a dose-dependent manner.

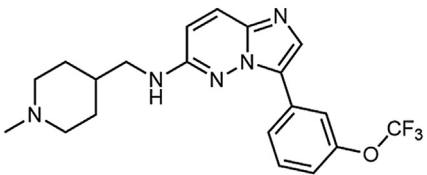
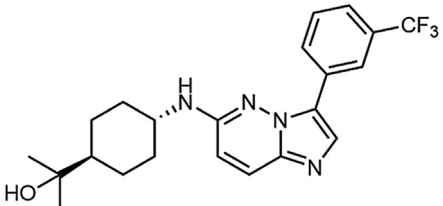
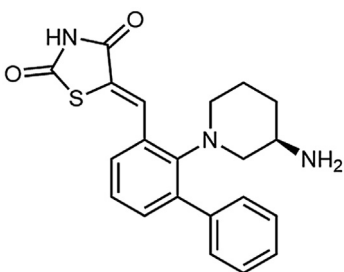
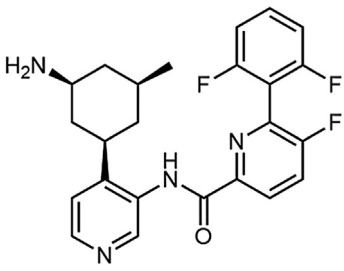
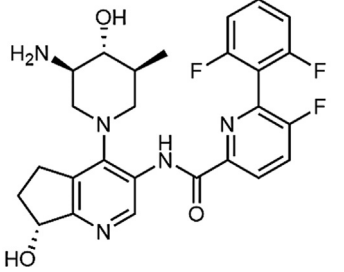
### Benzonaphthyridines

Pierre et al designed a class of pan-PIM kinase inhibitors by modifying the functional groups of compound **7** (**Fig. 2**), a CK2 inhibitor and also known as CX-4945.<sup>24</sup> It is worth noting that most of the structural changes on the C ring that reduced inhibitory activity against CK2 also affected PIM's inhibition. However, the extent of change was significantly lower for the latter enzymes in compounds bearing a carboxylate or a carboxamide moiety at 7-position. More interestingly, one H-bond donor in the carboxamide moiety is necessary to inhibit the protein; however, extension of the amides with bulkier groups decreased the activity. Aniline moieties (2'-chloro or 2'-fluoro aniline) at 5-position showed single-digit nanomolar potency against PIM kinases, and could sustain large solubilizing groups at 4'-position with retention of the potent activity. **8** was as effective as the triazole counterpart in inhibiting the PIM2 isoform, but slightly less potent against PIM1. Triazole derivative **9** revealed a noteworthy increase in potency with  $IC_{50}$  values of 5, 6, and 86 nmol/L against three isoforms of the enzyme respectively and inhibits the phosphorylation of BAD at Ser112 in MV4-11 with  $IC_{50}$  lower than 30 nmol/L.

### Triazolopyridines and Triazolopyridazines

Through structure-based virtual screening, Pastor et al identified 1,2,3-triazolo [4,5-*b*]pyridine as the scaffold for PIM inhibitors with the help of a scaffold hopping approach. Derivatives bearing piperidinyl-methyl amine at 5-position of **10** (ETP-46546) displayed the most active PIM1 inhibition within the first batch of triazolopyridine analogs (**Fig. 3**).<sup>25,26</sup> Molecular docking study revealed the binding mode and key interactions of **10** at the catalytic site of PIM1

**Table 1** Small-molecule pan-PIM inhibitors that have entered clinical trials

Compound	<i>In vitro</i> activity	Development status (organization)	Clinical trials in disease
<b>SGI-1776</b> 	$IC_{50}$ PIM1 = 7 nmol/L PIM2 = 363 nmol/L PIM3 = 69 nmol/L	Discontinued (Astex)	<ul style="list-style-type: none"> <li>▪ NCT01239108 (withdrawn); relapsed + refractory leukemias.</li> <li>▪ NCT00848601 (terminated); prostate cancer/non-Hodgkin's lymphoma.</li> </ul>
<b>TP-3654</b> 	$K_i$ PIM1 = 5 nmol/L PIM2 = 239 nmol/L PIM3 = 42 nmol/L	Phase I (Sumitomo Dainippon Pharma)	<ul style="list-style-type: none"> <li>▪ NCT03715504 (completed); advanced solid tumors.</li> <li>▪ NCT04176198 (recruiting); myelofibrosis.</li> </ul>
<b>AZD1208</b> 	$IC_{50}$ : PIM1 = 0.4 nmol/L PIM2 = 5 nmol/L PIM3 = 1.9 nmol/L	Phase I (AstraZeneca)	<ul style="list-style-type: none"> <li>▪ NCT01489722 (terminated); AML.</li> <li>▪ NCT01588548 (completed); advanced solid malignancies.</li> </ul>
<b>PIM447</b> 	$K_i$ PIM1 = 6 nmol/L PIM2 = 18 nmol/L PIM3 = 9 nmol/L	Phase I (Novartis)	<ul style="list-style-type: none"> <li>▪ NCT01456689 (completed); MM.</li> <li>▪ NCT02078609 (completed); AML and high-risk MDS.</li> <li>▪ NCT02144038 (completed); relapsed and refractory MM.</li> <li>▪ NCT02160951 (completed); MM.</li> <li>▪ NCT02370706 (completed); myelofibrosis.</li> </ul>
<b>INCB-053914</b> 	$IC_{50}$ PIM1 = 0.24 nmol/L PIM2 = 30 nmol/L PIM3 = 0.12 nmol/L	Phase I/II (Incyte)	<ul style="list-style-type: none"> <li>▪ NCT03688152 (completed); relapsed/refractory diffuse large B cell lymphoma.</li> <li>▪ NCT04355039 (withdrawn) relapsed/refractory MM.</li> <li>▪ NCT02587598 (terminated); solid tumors.</li> </ul>

Abbreviations: AML, acute myeloid leukemia; MDS, myelodysplastic syndrome; MM, multiple myeloma.

kinase (PDB code: 4A7C), and the results are presented in **Fig. 3**. There is one H-bond between the side chain of Lys67 and the nitrogen in the triazole ring. The aromatic ring is involved in the hydrophobic interaction formed with Phe49, Val52, and Leu174. The *m*-trifluoromethoxy group

creates an additional hydrophobic interaction with the hinge residue Pro123. By substituting the piperidine NH at 1-position or varying the distance from the amino group attached to the triazolopyridine scaffold, it is confirmed that the presence of an unsubstituted NH in the amine

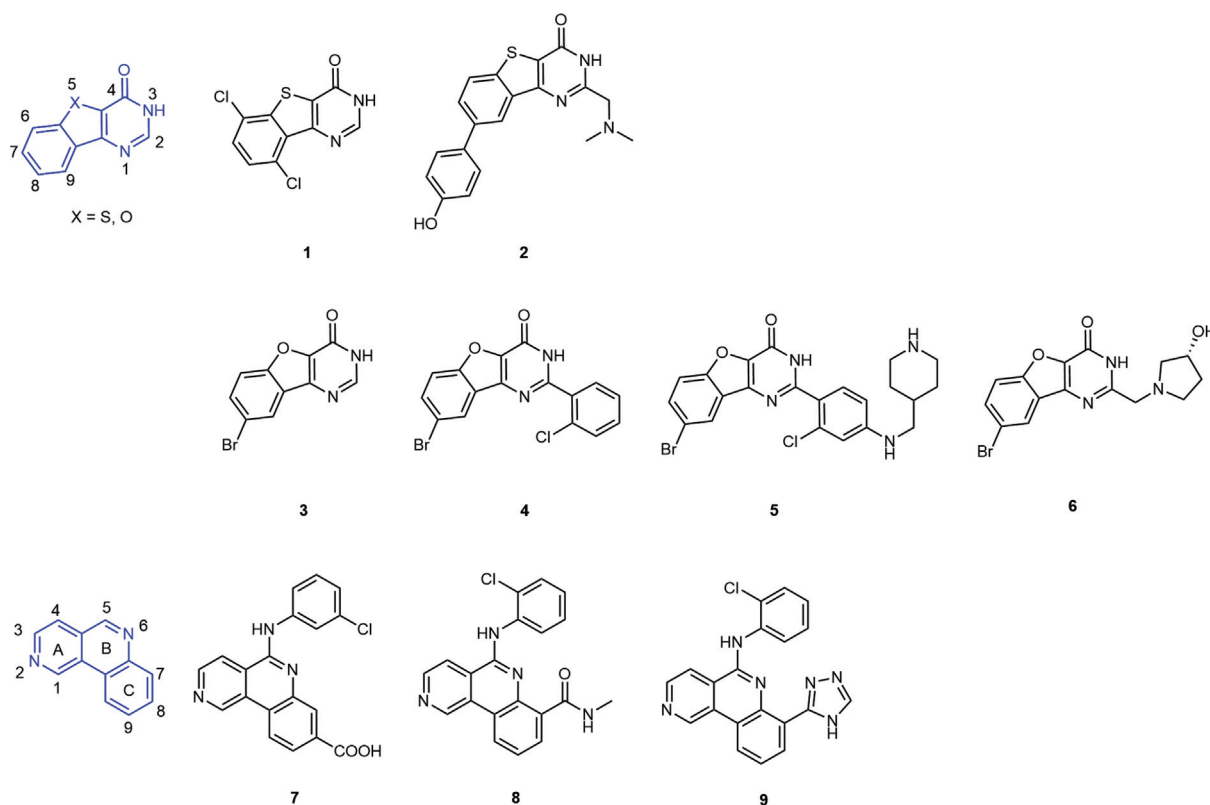


**Fig. 2** Representative compounds of benzothienopyrimidinone, benzofuroprymidinone, and benzonaphthyridines.

fragment was required for high PIM1 inhibitory potency.  $IC_{50}$  values of **10** were 6, 230, and 7 nmol/L toward PIM1, PIM2, and PIM3, respectively. Compound **11** (ETP-47453) showed improved PIM2 inhibitory activity over eightfold. When **11** was intravenous (iv) administered in BALB/C mice at 5 mg/kg, the plasmatic half-life is 0.95 hour and the plasmatic clearance is 3.28 L/h/kg.

Martínez-González et al performed computational modeling studies with early the lead compound and noticed that tricyclic derivative **12** could be easily accommodated in the catalytic site of the PIM1 protein by displacement of the P-loop when compared with **11** (►Fig. 3).<sup>27</sup> By forming a fused morpholinyl cycle at 6- and 7-positions, this chemical series of PIM inhibitors has mainly yielded a PIM1/3 profile with negligible PIM2 activity and high selectivity against a recurrent off-target of other PIM inhibitor families exemplified by **13**. Other isoform profiles such as **14** have been identified as pan-PIM inhibitors in enzymatic-based assays with  $IC_{50}$  values of 4, 27, and 6 nmol/L, respectively. After iv administration in BALB/C mice, the plasmatic clearance of **14** is 1.39 L/h/kg.

### Pyrrolopyrazinone

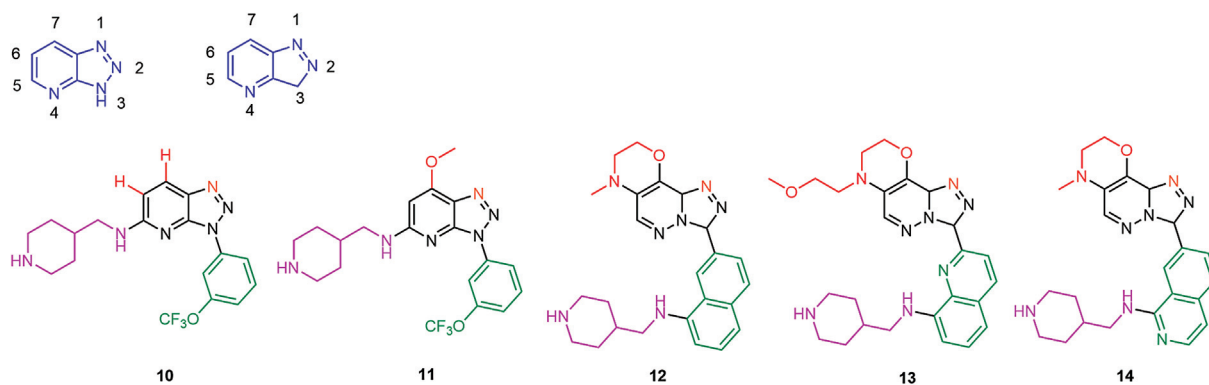
Inspired from natural product marine pyrrole alkaloids, Casuscelli et al synthesized a series of pyrrolo[1,2-*a*]pyrazinone derivatives.<sup>28,29</sup> Molecular docking study of PIM1 kinase (PDB code: 4BZN) with hit indicated that **15** did not form the classical pair or triplet of hydrogen bonds with the kinase

hinge region, therefore, high selectivity is observed across the kinase panel, as shown in ►Fig. 4. Preliminary analysis of the structure–activity relationship (SAR) indicated that the absence of the neopentyl hydrophobic group or its substitution with smaller alkyl groups caused significant loss of activity, thus, revealing the importance of lipophilic substituents in the binding of this enzyme. To enhance the druggability of **15**, a series of reasonably sized hydrophobic and hydrophilic substituents branch out into both  $R_1$  and  $R_2$  on the racemic scaffold. **16** was positively charged at physiological pH, therefore, it was still devoid of significant cellular activity owing to the poor permeability. Replacement of fluorine with chlorine **17** gave a threefold enhancement of affinity for PIM1 and twofold for PIM2, and the cellular activity reached  $IC_{50}$  values of 3, 73, and 12 nmol/L against three PIM kinases, respectively. Compound **17** had better kinase selectivity and exhibited good antiproliferative activity to MV4–11, LP-1, LNCaP, and CAPAN-1 cell lines with  $IC_{50}$  values of 1.5, 1.9, 3.3, and 3.7  $\mu$ mol/L, respectively.

### Thiazolidinedione

Beharry et al explored a series of benzylidene thiazolidine-2,4-diones (TZDs) that function as potent PIM protein kinase inhibitors.<sup>30,31</sup> These compounds blocked the ability of PIM to phosphorylate peptides and proteins *in vitro* with  $IC_{50}$  values in the nanomolar range, and substrates 4E-BP1 and p27<sup>Kip1</sup> were directly involved in the phosphorylation of PIM kinase *in vitro*. Molecular docking study of **18** (SMI-4a) with





Binding mode illustrated in different colors: P-loop oriented fragment, Asp128-solvent area, hinge area, hydrogen bonded with Lys67.

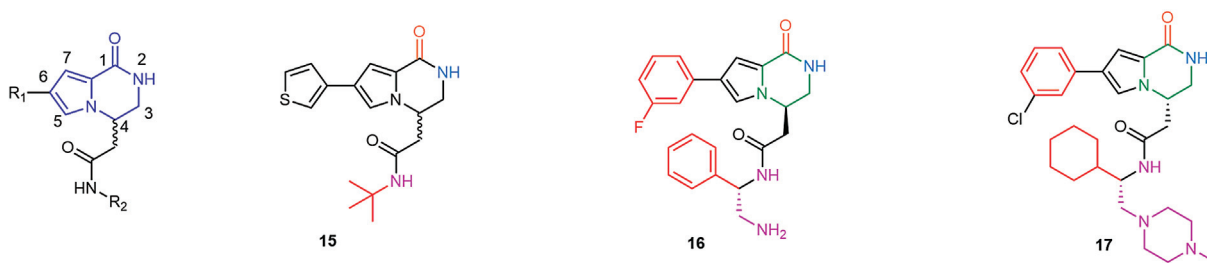
**Fig. 3** Representative compounds of triazopyridines and triazopyridazines. Illustration: the molecular interaction of **10–14** with PIM1 kinase appears in different colors.

PIM1 kinase (PDB code: 1XWS) suggested that the thiazolidine NH group donates a hydrogen bond to the carbonyl oxygen of Glu121, and the trifluorophenyl group makes numerous van der Waals contacts with the hydrophobic cleft (**Fig. 5**). Compound **19** (SMI-16a) effectively prevents bone destruction while suppressing tumor growth in multiple myeloma (MM) animal models.<sup>32</sup> Treatment with PIM2 short-interference RNA as well as SMI-16a successfully restores osteoclastogenesis suppressed by some inhibitory factors and MM cells. SMI-16a also suppresses the drug-efflux function of breast cancer resistance protein. Fujii et al clarified that TZD family compounds destroyed clone formation in MM cells, and their tumorigenic ability *in vivo* under acidic conditions.<sup>33</sup>

Dakin et al used HTS to confirm **20** as a hit against PIM2, with an  $IC_{50}$  value of 0.16  $\mu\text{mol/L}$ .<sup>34</sup> In consideration of the poor PK and drug-like properties of phenols, a series of active TZDs were synthesized via Knoevenagel condensation. Incorporation of hydrophobes at R2 position afforded inhibitors approaching the limit of detection of Km [ATP] enzyme assays against all PIM isoforms, as **21** and **22** exhibited (**Fig. 5**). Preliminary docking information hints that the aromatic core including acidic TZD and basic amine involved

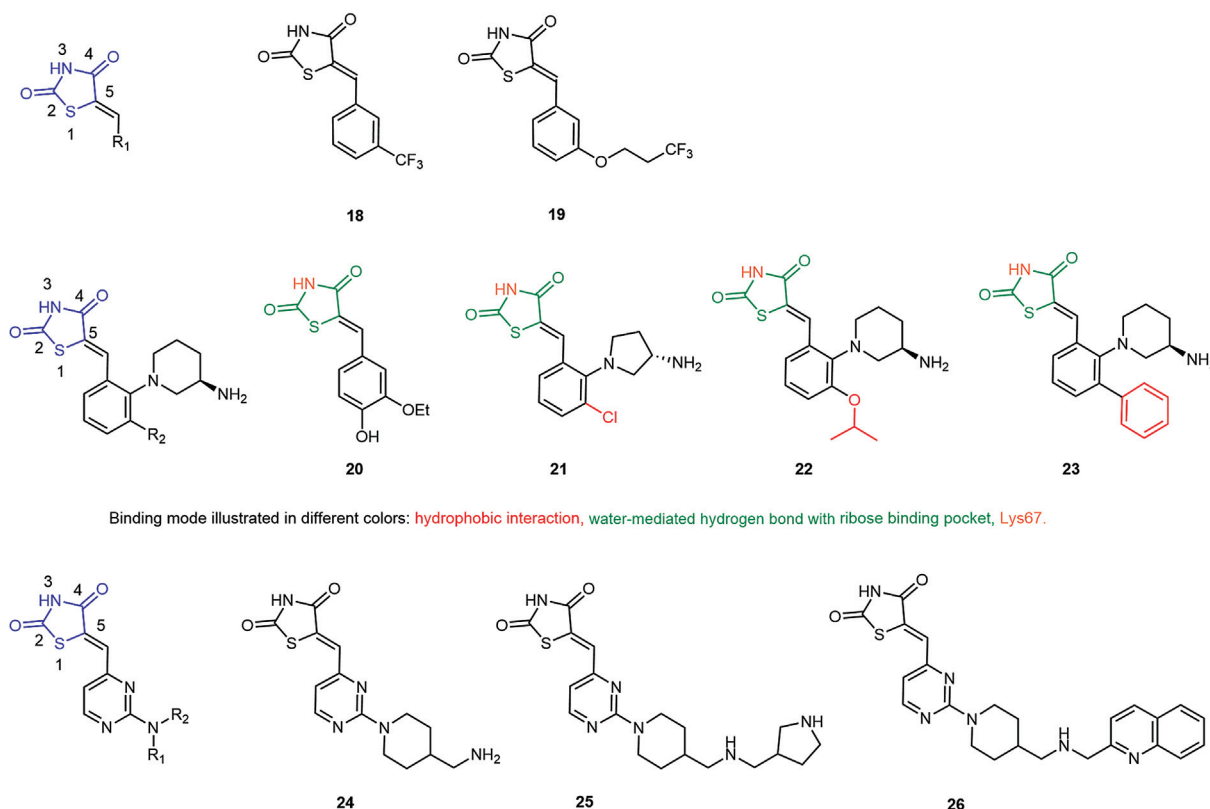
in interacting with the carboxylate-rich ribose-binding pocket and conserved Lys67 separately, as shown in **Fig. 5**. The binding mode is also confirmed by the X-ray crystal structure of **22** in PIM1 (PDB code: 3BGQ). To achieve an approximate intracellular concentration, some leading examples were evaluated in enzyme assays with high substrate concentrations. Additionally, these inhibitors have been demonstrated to have good antiproliferative activity in the MOLM-16 cell line with  $GI_{50}$  values below 100 nmol/L. The efficacy of **23** (AZD1208) in cultured acute myeloid leukemia (AML) cell lines, tumor xenograft models, and *ex vivo* cultures of primary tumor cells from Flt3-ITD and Flt3 wild-type patients is demonstrated, as well as accompanying modulation of PIM signaling substrates that can contribute to the inhibition of tumor growth.<sup>35</sup> Phase I trials were completed for **23**, but the study was terminated while the drug was being tested for safety, tolerability, PKs, and efficacy in AML patients; the reason was not disclosed.<sup>36,37</sup>

Flanders et al designed to incorporate a diamine component into the TZD molecule and described a class of potent pan-PIM inhibitors exhibiting micromolar  $IC_{50}$ .<sup>38</sup> The length, position, and basicity of the terminal NH group in compound **24** play an important role in the enzymatic activity, whereas



Binding mode illustrated in different colors: hydrophobic interaction, hinge area, hydrogen bonded with Lys67, hydrogen bonded with Asp186, water-mediated hydrogen bond with ribose binding pocket (Asp128 side chain and the backbone carbonyl of Glu171).

**Fig. 4** Representative compounds of pyrrolopyrazinones. Illustration: the molecular interaction of **15–17** with PIM1 kinase appears in different colors.



Binding mode illustrated in different colors: hydrophobic interaction, water-mediated hydrogen bond with ribose binding pocket, Lys67.

**Fig. 5** Representative compounds of thiazolidinedione derivatives. Illustration: the molecule interaction of 20–23 with PIM1 kinase appears in different colors.

when it was replaced with pyrrolidin-3-ylmethyl, the  $IC_{50}$  value was substantially decreased by  $\sim 10$ -fold compared with **25**. Given the poor permeability of **24** as measured in PAMPA assay, researchers explored the incorporation of aromatic groups attached to the end of the molecule for the purpose of increasing hydrophobicity while retaining the basic NH moiety at the same position as that in **24**. Compound **26** was determined to have  $IC_{50}$  values of 13, 15, and 15 nmol/L against three PIM kinases and also demonstrated a clear selectivity profile across a panel of 150 oncology relevant kinases when screened at 0.5  $\mu\text{mol/L}$ . Dosing the rats with 5 mg/kg of **26** intravenously and orally demonstrated a plasma half-life of 3.1 hours with very good oral bioavailability.

### Rhodanine Derivatives

Bataille et al identified **27** as a starting point though HTS ( $\rightarrow$  Fig. 6).<sup>39</sup> A range of aryl and heteroaryl derivatives were readily available based on Knoevenagel condensation between rhodanine and corresponding aldehydes. The binding mode with **28** against PIM1 (PDB code: 2C31) is demonstrated in  $\rightarrow$  Fig. 6. The oxygen on the rhodanine head group formed a hydrogen bond interaction with the water molecule, which tightly associated with the Lys67 residue. Besides, substitution on the aryl ring is well tolerated in biological activities, either introducing a strong electron-donating group or a -withdrawing group; however, the poor solubility of this series limited further

development in this case. On the one hand, researchers further designed a range of fused tricyclic scaffolds which could potentially interacted in a bioisosteric way, but improvement was not desirable because of the metabolic instability of thiocarbonyl in rhodanine. On the other hand, replacement of the rhodanine head group with a pseudo-thiohydantoin was confirmed to increase metabolic stability. In this work, the most potent compound **29** (OX0642) gave an  $IC_{50}$  of 3.4  $\mu\text{mol/L}$  against MV4-11 cells and 0.75  $\mu\text{mol/L}$  against K562 cell lines ( $\rightarrow$  Fig. 6).

On this basis, Quevedo et al used **29** as a benchmark for further optimizations through a structure-based design strategy to synthesize **30** (OX0099) ( $\rightarrow$  Fig. 6).<sup>40</sup> Based on the CEREP express assay results, it was deemed that the presence of *N*-methyl piperidine head group was associated with high levels of efflux and substantial off-target toxicity. Among this series of compounds, complete removal of the basic *N*-methyl and addition of a hydroxyl group **31** (OX1399) resulted in a better hERG profile and simultaneously much lower efflux ratios.

Sawaguchi et al identified a rhodanine-benzylidene derivative **32** in screening of PIM1 inhibitor, followed by the discovery of **33**, a highly potent and selective pan-PIM inhibitor ( $\rightarrow$  Fig. 6).<sup>41</sup> **33** inhibited PIM1, PIM2, and PIM3 kinase activities with  $IC_{50}$  values of 16, 13, and 6.4 nmol/L, respectively, and induced cell-cycle arrest and apoptosis at the G1 phase against both PC-3 and MV4-11 cells in dose-dependent manners from 0.3 to 10  $\mu\text{mol/L}$ .

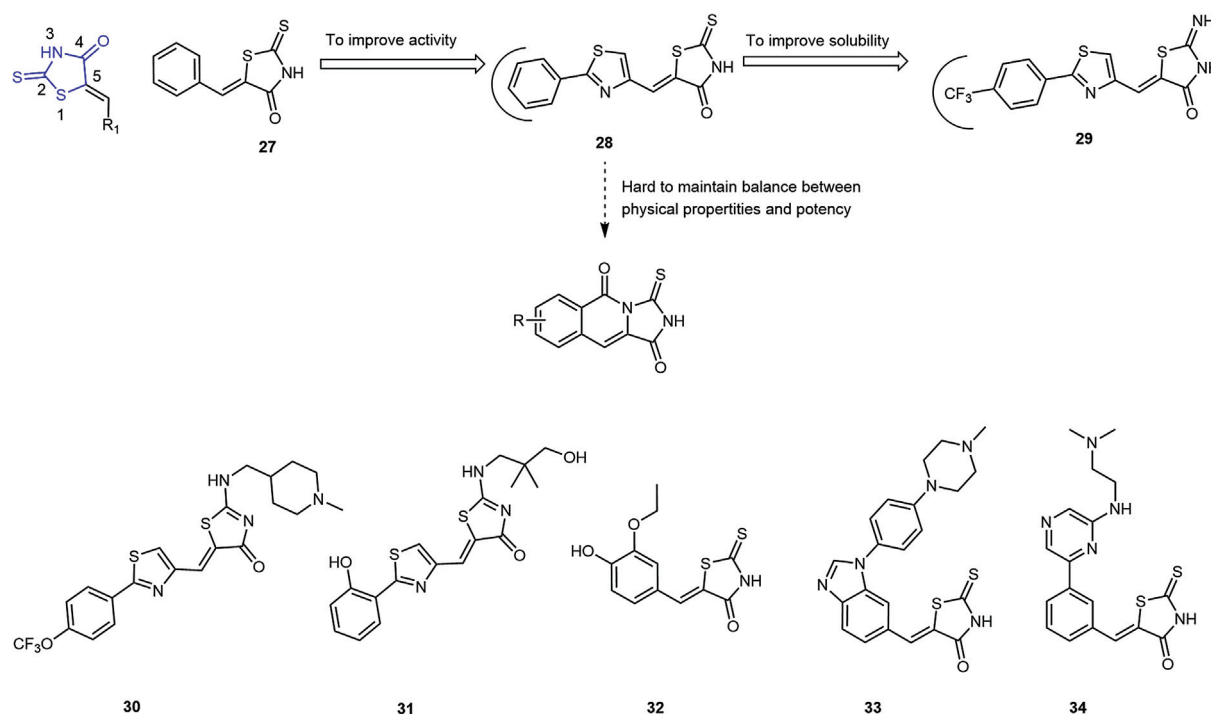


**Fig. 6** Representative compounds of rhodanine derivatives.

Lee et al synthesized 2-thioxothiazolidin-4-one derivatives.<sup>42,43</sup> Taking **34** as an example,  $IC_{50}$  values of the compound were 1, 7, and 1 nmol/L against all three PIM kinases. The compound inhibited the growth of MOLM-16 cell lines and modulated the expression of pBAD and p4EBP1 in a dose-dependent manner. The antiproliferative activity of the rhodanine against EOL-1 and MOLM-16 cells was much higher than that of TZD counterparts (**Fig. 6**).

### Pyridyl Carboxamide

Burger et al described hit optimization efforts that were initiated by variation of three components of compound **35** including piperidine, phenyl, and NH-acetyl thiazole (**Fig. 7**).<sup>44</sup> Molecular docking study of the compound in PIM1 kinase (PDB code: 4N6Y) exhibited that **35** did not form any hydrogen bond with the hinge or any other part of protein; therefore, further optimization was proceeded by improving potency with minimal increase in lipophilicity and overall drug-like properties. Compound **36** (LGB321) showed high kinase selectivity against three PIM members with  $K_i$  values of 0.001, 0.002, and 0.001 nmol/L, respectively. Molecular docking of **36** in PIM1 kinase (PDB code: 4N70) indicated that amino group to Asp128 side chain and Glu171 backbone carbonyl, and pyridyl to Lys67 participate in three hydrogen bonds to the protein. Compound **36** demonstrated significant inhibitory activity and selectivity in both enzymatic and cell-based assays with encouraging results in an EOL-1 AML xenograft mouse model.<sup>45</sup>

Burger et al focused on the improvement of metabolic stability for the pyridylamide scaffold.<sup>46</sup> **37** (PIM447,

LGB447) is a potent and selective pan-PIM kinase inhibitor, derived from **36** (**Fig. 7**).  $K_i$  values of **37** were 0.006, 0.018, and 0.009 nmol/L for PIM kinases, respectively. **Fig. 7** illustrates the binding interactions of **37** with PIM1 kinase (PDB code: 5DWR). Thirteen Japanese patients with relapsed and/or refractory MM were enrolled in the phase I study of **37** (NCT02160951). However, due to early termination of the study, maximum-tolerated dose and recommended dose for the drug were not determined. When **37** was orally administered at doses of 250 and 300 mg once daily on 28-day continuous cycles, it was tolerated with an overall response rate of 15.4% and a disease completed response of 69.2%.

Nishiguchi et al further designed and synthesized several combinations of A/B rings with more polar C/D rings, with the goal of lowering the cLogP into a range of 1 to 2.<sup>47</sup> A representative example is shown as **38**. An X-ray co-crystal structure in PIM1 was obtained (PDB code: 5IIS).

Koblish et al reported the initial preclinical characterization of pan-PIM inhibitor compound **39** (INCB053914), as shown in **Fig. 7**.<sup>48</sup> Compound **39** potentially inhibited the activities of all three PIMs with  $IC_{50}$  values of 0.24, 30, and 0.12 nmol/L, respectively. Single-agent INCB053914 inhibited phosphorylation of Bcl-2-associated death promoter protein and tumor growth in AML and MM xenografts in a dose-dependent manner. Additionally, INCB053914 at low nanomolar concentrations enhances the efficacy of ruxolitinib in inhibiting the neoplastic growth of primary MPN patient cells and antagonizes persistent myeloproliferation of ruxolitinib *in vivo*.



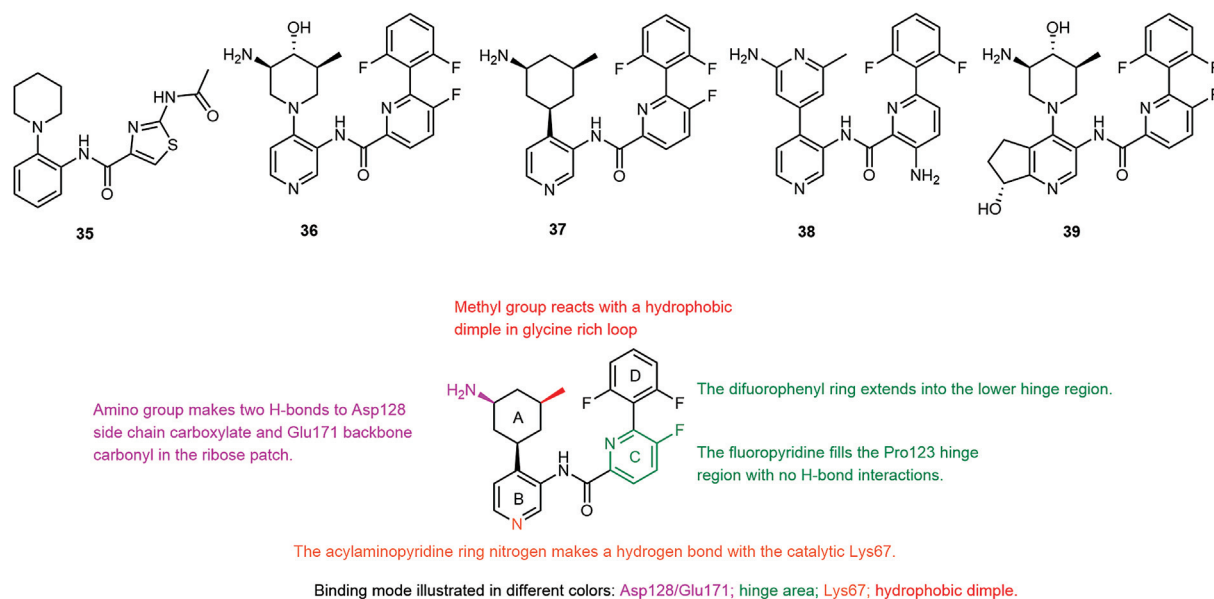


**Fig. 7** Representative compounds of pyridyl carboxamide derivatives. Illustration: the molecular interaction of PIM447 with PIM1 kinase appears in different colors.

### Diaminopyrazole

Ishchenko et al identified **40** and **41** (►Fig. 8) as potential pan-PIM inhibitors.<sup>49</sup> The  $IC_{50}$  value of *S* stereoisomer **40** against three PIM kinases was 5 to 20-fold potency than that of *R* stereoisomer counterpart **41**. The crystal structure presented that direct hydrogen bond interactions to Asp128 and Glu171 in **40** was not necessary for strong inhibition. The replacement of pyrrolidine with other types of functional groups led to the loss of activity in PIM2. With the use of computer-aided drug design, docking confirmed amide in **42** as a driving force to achieve low-energy bound conformation through intramolecular hydrogen bonds to the thiazole nitrogen and the ether linker. **42** had improved inhibitory activity against three PIMs with  $IC_{50}$  being 1 nmol/L for all three.

Wang et al modified Burger et al's work and prepared **43** in which the 3-aminopyridine was replaced by a bioisosteric 5-aminothiazole group (►Fig. 8).<sup>50</sup> To mitigate potent liabilities including hERG inhibition, the use of a diaminopyrazole moiety in place of the diaminopyridine in **43** gave compound **44**, which combined the best properties of **43** and previous study in terms of potency and solubility. The co-crystal structure of **44** in complex with PIM1 kinase (PDB code: 5V80) was released. However, further development of **44** is limited because of the poor *PK* properties, and the mono-fluoro-substitution at the  $\beta$ -position of the primary amine led to the generation of compound **45** (GDC-0339). The binding mode and interactions of **45** bound to PIM1 kinase (PDB code: 6N09) are visualized in ►Fig. 8. Compound **45** is an orally bioavailable and well-tolerated pan-PIM kinase inhibitor with demonstrated efficacy in RPMI8226 and MM.1S human MM xenograft mouse models. The ADME properties were anticipated to be moderate in human. Besides, GDC-0339 is active in MM cancer cells both as a single agent and in combination with PI3K inhibitor GDC-0941.

### Pyrazolopyrimidine

Through virtual screening, Wang et al selected **46** as lead compound with extensive hit triage on PIM potency and ligand efficiency (►Fig. 9).<sup>51</sup> The binding mode of the PIM1 kinase domain (PDB code: 4K0Y) with **46** is shown in ►Fig. 9. The piperidine nitrogen found in **46** has a calculated  $pK_a$  of 9.75, while the hydroxyl group at 7-position has a calculated  $pK_a$  of 5.9. The existence of **46** under physiological conditions may be associated with low cell permeability and oral bioavailability. To improve the PIM potency while maintaining high ligand efficiency, the removal of oxygen at 4-position of the pyrazolopyrimidone core may facilitate the interaction of the basic amine with the acidic patch. Thus, a series of structure-based modifications were conducted at  $R_1$ ,  $R_2$ , and  $R_3$  positions, and further optimizations on  $\beta$ -fluoro-substitution in the piperidine ring gave **47** with ~10,000-fold inhibitory improvement on PIM2. Also, more lipophilic contacts were further observed in a co-crystal structure of human PIM1 kinase (PDB code: 4K1B) and **47**, as shown in pink. **47** has a potency of 0.15  $\mu\text{mol/L}$  against BaF3\_Pim1 cells and inhibited the MM1.S cell line with an  $IC_{50}$  of 1.9  $\mu\text{mol/L}$ .

Dwyer et al conducted modifications of C5 and C3 of the pyrazolo[1,5-*a*]pyrimidine core to enhance *in vitro* potency against PIM1 as well as other family members, preferentially PIM2.<sup>52,53</sup> Initial HTS screening identified **48** as an early hit (►Fig. 9). Pyridyl at the C5 position was replaced with an ethylenediamine group to enhance PIM1 and PIM2 potency and the C3 position was introduced into the generally well-tolerated heterocyclic ring such as 1,2,4-oxadiazole to obtain a series of derivatives including **49**. Compound **49** demonstrated *in vitro* activity versus PIM1, PIM2, and PIM3 with  $IC_{50}$  values of 1.3, 7.3, and 1.8 nmol/L, respectively. It was found to be clean in both cytochrome P450 evaluation and hERG ion channel evaluation.

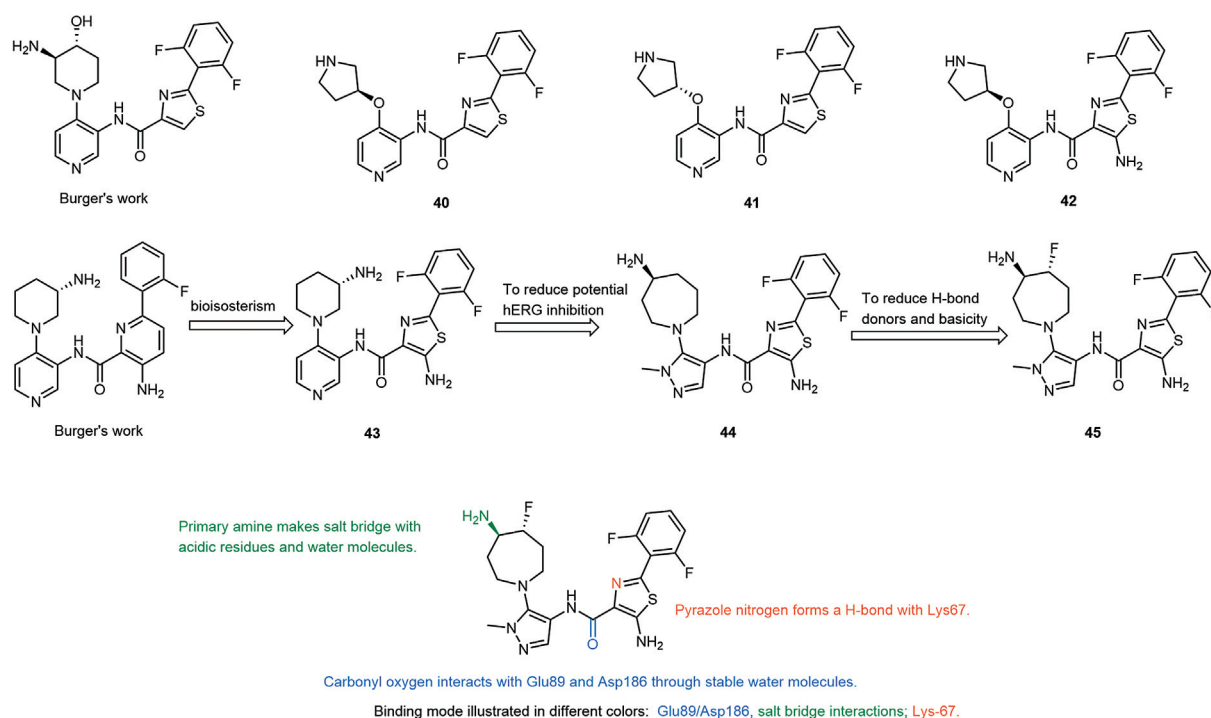


**Fig. 8** Representative compounds of diaminopyrazole derivatives. Illustration: the molecular interaction of GDC-0339 with PIM1 kinase appears in different colors.

However, additional evaluation of this class of PIM inhibitors was not disclosed.

Foulks et al retained the pyrazolo[1,5-*a*]pyrimidine core of **50** (SGI-1776), while the 3,5-position was modified to generate the second-generation PIM kinase inhibitor **51** (TP-3654),<sup>54</sup> which remains a potent pan-PIM inhibitor but with minimal to no inhibition of hERG and cytochrome P450 as observed with **50**. Compound **51** (1  $\mu\text{mol/L}$ ) displays at least 10-fold or greater selectivity for PIM1 compared with other kinases tested. Researchers evaluated the efficacy of **51** against several urothelial carcinoma cancer cell lines, including T24, UM-U3C, RT4, and J82 with  $\text{EC}_{50}$  values ranging from 0.82 to 3.54  $\mu\text{mol/L}$ . When rats were administered with **51** (iv, 2 mg/kg; 40 mg/kg, orally), the  $T_{\text{max}}$  value of the drug was 1 hour, with a half-life of 4.1 hours.

### 3,5-Disubstituted Indole

Nishiguchi et al identified hit **52** via internal HTS (**Fig. 10**).<sup>55</sup> The binding mode indicated that the N-H of the 1*H*-pyrazolo[3,4-*b*]pyridine core makes a hydrogen bond to the hinge. The hydroxyl group of the phenol acts as a hydrogen bond donor to Glu89 and a hydrogen bond acceptor from the backbone amide of Phe187. Compound **52** has pan-PIM inhibitory activity with  $\text{IC}_{50}$  values of 9, 39, and 12 nmol/L, but can also significantly inhibit c-kit, PDGFR, KDR, and other kinases. In consideration of the potentially metabolic liability, a survey of phenol replacements was investigated on the 1*H*-pyrazolo[3,4-*b*]pyridine core, but none of these derivatives were as potent as the phenol. Therefore, researchers considered to alternate the scaffold of 7-azaindazole with disubstituted indole, which not only

retained the potency but also enhanced selectivity against the target kinases. The highly selective indole chemotypes, such as *S*-enantiomer **53**, exhibited potent nanomolar PIM2 enzymatic inhibition with an  $\text{IC}_{50}$  value of 12.2 nmol/L.

More et al modified the 5-position of meridianin C to obtain a series of PIM kinase inhibitors (**Fig. 10**).<sup>56</sup> Compound **54** exhibited the best activity with  $\text{IC}_{50}$  values of 3.4, 110, and 6.5 nmol/L, respectively, and has good selectivity against a variety of kinases, but showed no significant inhibitory activity on leukemia cell lines MV4-11, K562, and Jurkat, and this may be due to its poor ability to penetrate the cell membrane. Interestingly, its physical and chemical properties were improved by substituting the 2-aminopyrimidine ring with a benzene ring and introducing different substituents into the benzene ring.<sup>57</sup> The combination of cyan and amine groups in *meta*- and *para*-positions, respectively, enhanced the synergistic inhibitory activity for all three PIM isoforms. Based on the docking stimulation study (PDB code: 5DWR), **55** formed two hydrogen bonds between the indole moiety and the carbonyl group of Glu121 and between the pyrazine moiety and Lys67. **55** inhibited three PIM kinases with  $\text{IC}_{50}$  values of 5, 259, and 10 nmol/L, respectively. The growth inhibitory activity of **55** against the leukemia cell line MV4-11 exhibited an  $\text{IC}_{50}$  value of 0.8  $\mu\text{mol/L}$ .

### Oxindole

Haddach et al identified hit **56** through HTS which inhibited PIM1 with an  $\text{IC}_{50}$  value of 386 nmol/L (**Fig. 11**).<sup>58</sup> The lactam NH and carbonyl of oxindole were deemed to interact with Lys67 and Asp186 in PIM1. The carboxylate moiety was

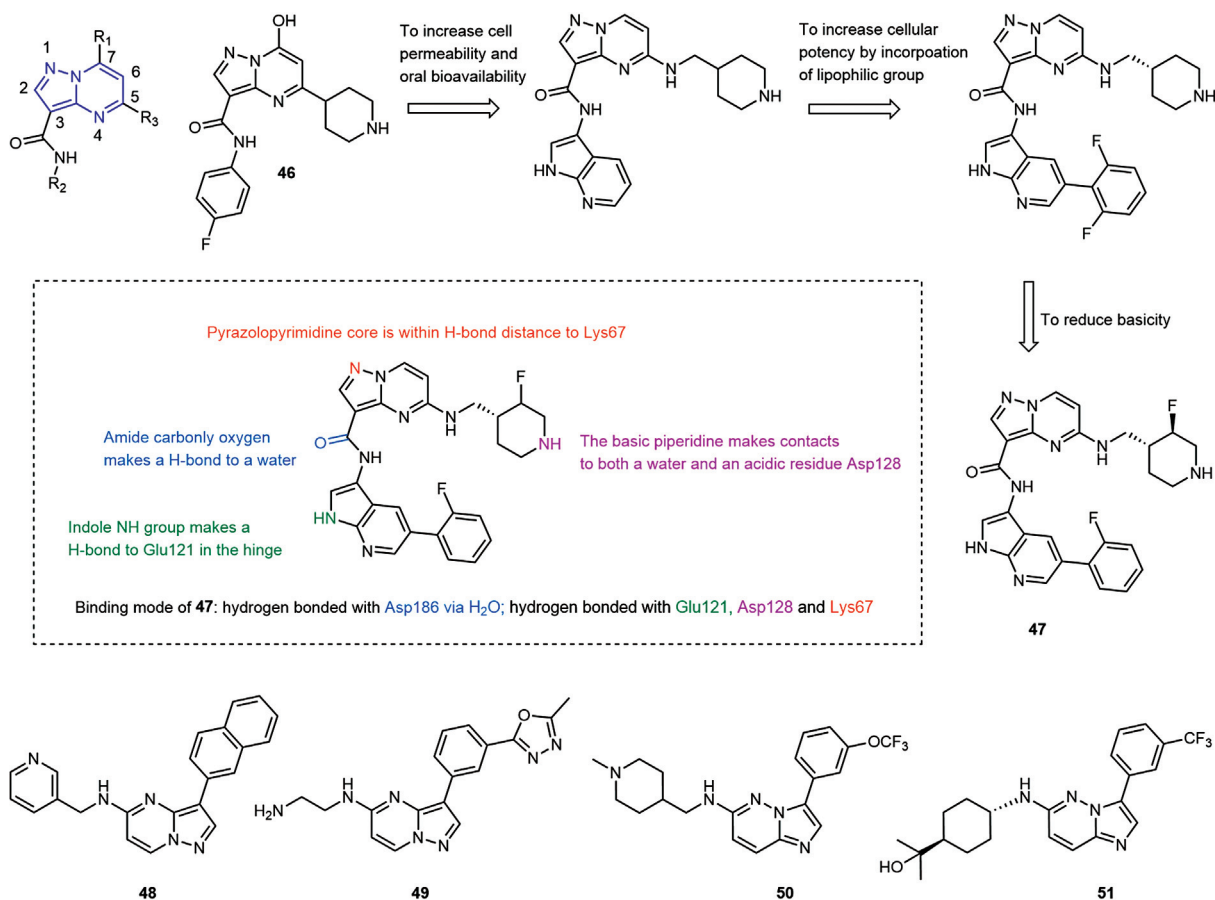


**Fig. 9** Representative compounds of pyrazolopyrimidine derivatives. Illustration: the molecular interaction of 47 with PIM1 kinase appears in different colors.

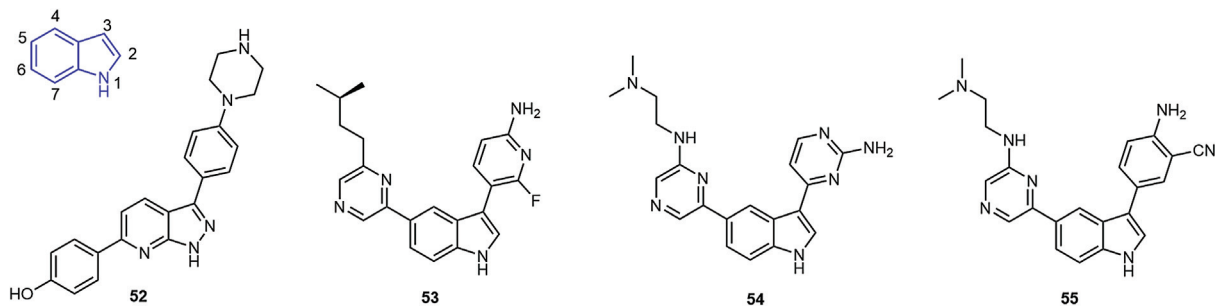


**Fig. 10** Representative compounds of 3,5-disubstituted indole derivatives.

considered as an appropriate position to incorporate polar groups. Methylation of 1-position of the oxindole, on the nitrogen atom, leads to loss of activity, and adding aliphatic basic amines to 56 via amide coupling led to an increase in potency at inhibiting PIM1 kinase, as shown as 57. Moreover, the basicity and rigidity of the side chain resulted in potent inhibition of both PIM1 and PIM2. Introduction of a chloro group at the 7-position caused a loss of potency against both enzymes, signifying the importance of coplanarity between the phenyl and furan rings. Of note, 58 (CX-6258) not only has good activity *in vitro* but also demonstrated a moderate PK profile. 58 has synergistic activity with chemotherapeu-

tics *in vitro* and enhances efficacy in both MV4-11 and PC3 tumor xenograft models. Treatment of mice bearing MV4-11 xenografts at oral doses of 50 and 100 mg/kg once daily was well tolerated and produced 45 and 75% tumor growth inhibition, respectively. Wang et al developed a multi-step synthetic route for the synthesis of the radio-labeled 59, which is profiled as a new PET (positron emission tomography) agent for imaging of PIM kinases in cancer.<sup>59</sup> Rebello et al reported that CX-5461, an orally bioavailable inhibitor of RNA polymerase I transcription, in combination with 58 showed significant efficacy in an MYC-driven autochthonous prostate cancer model.<sup>60</sup> Zheng et al first reported a

synergistic antimyeloma effect of the combination of **58**, SGI1776, and lenalidomide, and the enhanced degradation of IKZF1 and IKZF3 through the regulation of cereblon protein expression.<sup>61</sup>

### Azaindoles

Hu et al screened and selected **60** as a lead compound, an Akt inhibitor with moderate PIM potency (–Fig. 12).<sup>62</sup> Molecular docking of **60** as an inhibitor of full length of PIM1 kinase (PDB code: 5DGZ) illustrated several polar interactions in the ATP-binding site, including a single hydrogen bond interaction with the hinge residue Glu121, a contact of the pyridine nitrogen with the catalytic Lys67, and multiple interactions of the primary amine with Glu171, Asn172, and Asp186. Researchers optimized a series of core motifs by monitoring changes in LipE and assembled 6-azaindazole derivatives from three directions. Molecular docking of **61** in a PIM1 kinase-active site (PDB code: 5DIA) is shown. SAR demonstrated that the basic amine was critical for potency by donating the active hydrogen to interact with the acidic residues or water. **62** is the most balanced profile in terms of potency and stability *in vivo* of this series, and showed potent antiproliferative activity with an IC<sub>50</sub> value of 0.64 μmol/L in cell-based assay against MM1.S. However, the poor bioavailability and high intestinal metabolism indicated by the MDCK measurements of **62** is a problem that needed to be addressed.

Wang et al discerned that glucuronidation for the 6-azaindazole analog is a major intestinal metabolic pathway, and hypothesized that the 6-azaindazole core may be associated with metabolic liability. Although compounds **63–66** have drug-like physicochemical properties, their bioavailability in rats is close to zero (–Fig. 13).<sup>63</sup> To improve both PIM potency and rat intestinal metabolism, a series of analogs with modified cores were synthesized, among which **67** (GNE-955) had a moderate rat clearance at 34 mL/min/kg with good oral exposure *in vivo*. **67** regulated phosphorylation levels of BAD and 4E-BP in MM.1S cells in a dose-dependent manner. In addition, **67** showed moderate inhibitory activity on hERG, which has higher safety than SGI-1776.

Wang et al described their developmental work from **68**, a derivative of indazole, to pan-PIM inhibitor **69** (–Fig. 14).<sup>64</sup> **68** possessed a single-to-double digit nanomolar range of

pan-PIM potency, with IC<sub>50</sub> values of 3, 70, and 4 nmol/L, respectively. The X-ray co-crystal structure of hit bound to PIM kinase (PDB code: 4RPV) revealed that the NH group of indazole forms a hydrogen bond with Glu121 in the hinge region. The nitrogen in the pyrazine ring forms a hydrogen bond with catalytic Lys67. The amino group on the piperidine ring interacts with acidic amino acids Asp186 and Asn172 via a salt bridge. By optimizing the fragment of the piperidine ring, (*S*)-isomer **69** was obtained with the most potent overall PIM potency of this series. The X-ray crystal structure of **69** in PIM1 (PDB code: 4WRS) showed that its axial alkoxy conformation possibly represented a low-energy conformer of the piperidine ring. It has weak hERG inhibitory activity, good liver microsome stability, and oral bioavailability (*F* = 89%). Besides, incorporation of polar functionality, such as an amino group or amide group, at 4-position of the 2-fluorophenyl ring resulted in **70** and **71**, which had a lower overall cLogP, decreasing from 5.3 to 4.2 and 3.8 separately.

7-Azaindole has been incorporated as a hinge-binding element in the design of many kinase inhibitors.<sup>65,66</sup> Unlike reports of co-crystallization of 7-substituted azaindoles at the active site of PAK1 kinase, the donor–acceptor motif of **72** faces away from the hinge site, and it is chlorine atom at 4-position of the ring that points to the part of the binding pocket (PDB code 5TEL) (–Fig. 15).<sup>67</sup> Barberis et al targeted the ribose binding pocket to improve PIM2 potency.<sup>68</sup> The crystal structure of **73** with PIM1 kinase (PDB code 5KCX), determined by X-ray, defines that chlorine at 4-position provides an atypical hinge contact with Glu121, and the carboxamide at 6-position interacts with Lys67. To better target the ribose-binding pocket, substitutions were introduced at 1-position, and it was shown that basic nitrogen-containing compounds, especially cyclohexyl or piperidinyl rings, exhibited notably good potency for PIM2. SAR showed that substitution at 3-position had to be a small hydrophobic group that maintains pan-PIM inhibition with reasonable cellular potency. For the purpose of investigating diverse chemical entities aimed at improving primarily physicochemical properties, bioisosteric replacement of the iodine was conducted. Of note, cyclopropyl alkyne derivative **74** displayed a moderate clearance and volume of distribution *in vivo* of PK properties.

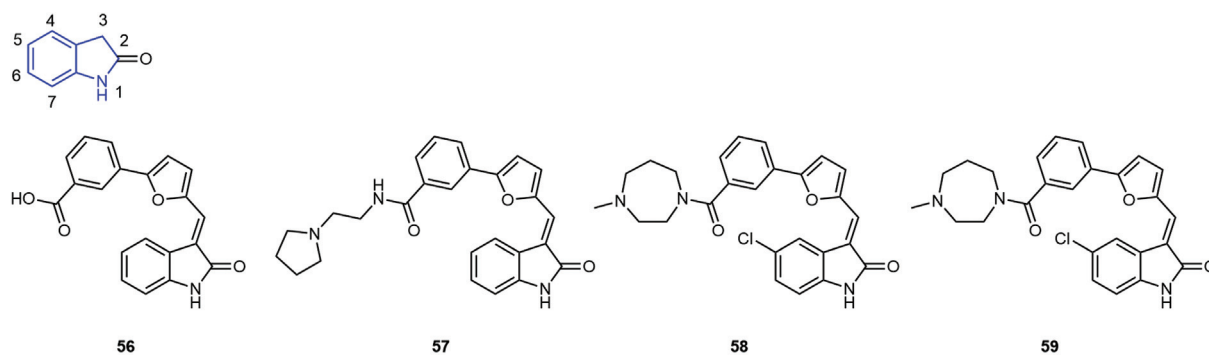


**Fig. 11** Representative compounds of oxindole derivatives.

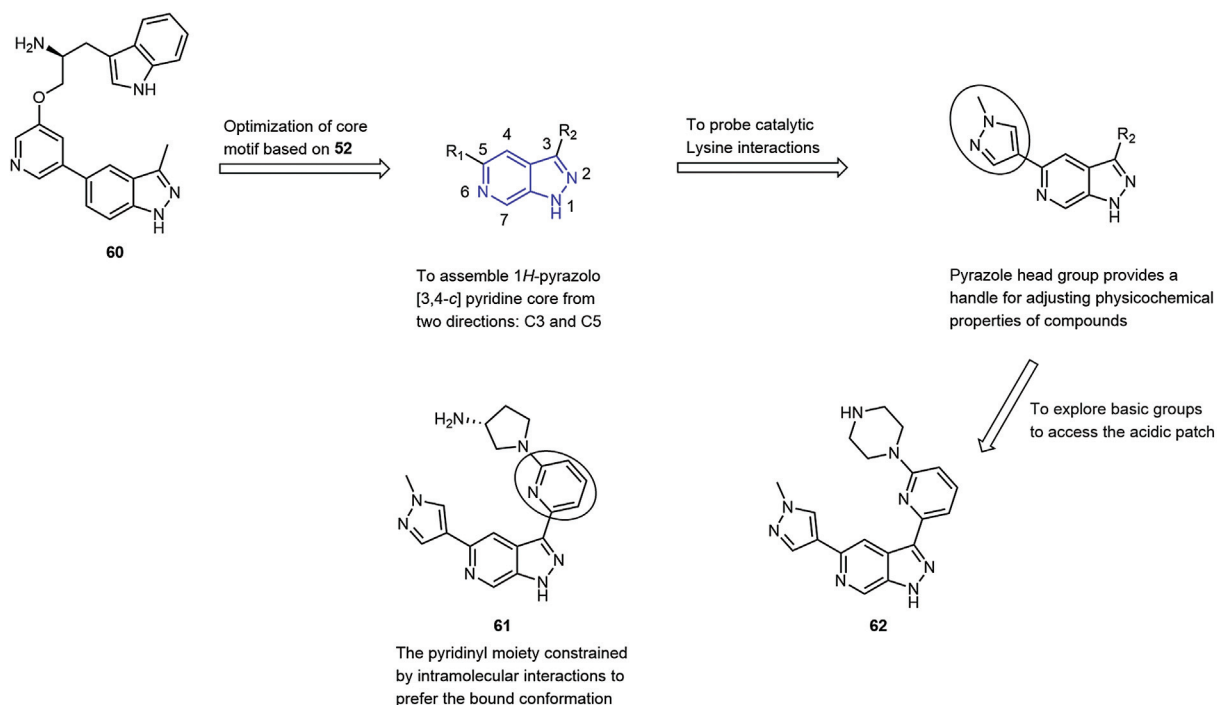


**Fig. 12** Representative compounds of 6-azaindazole derivatives.

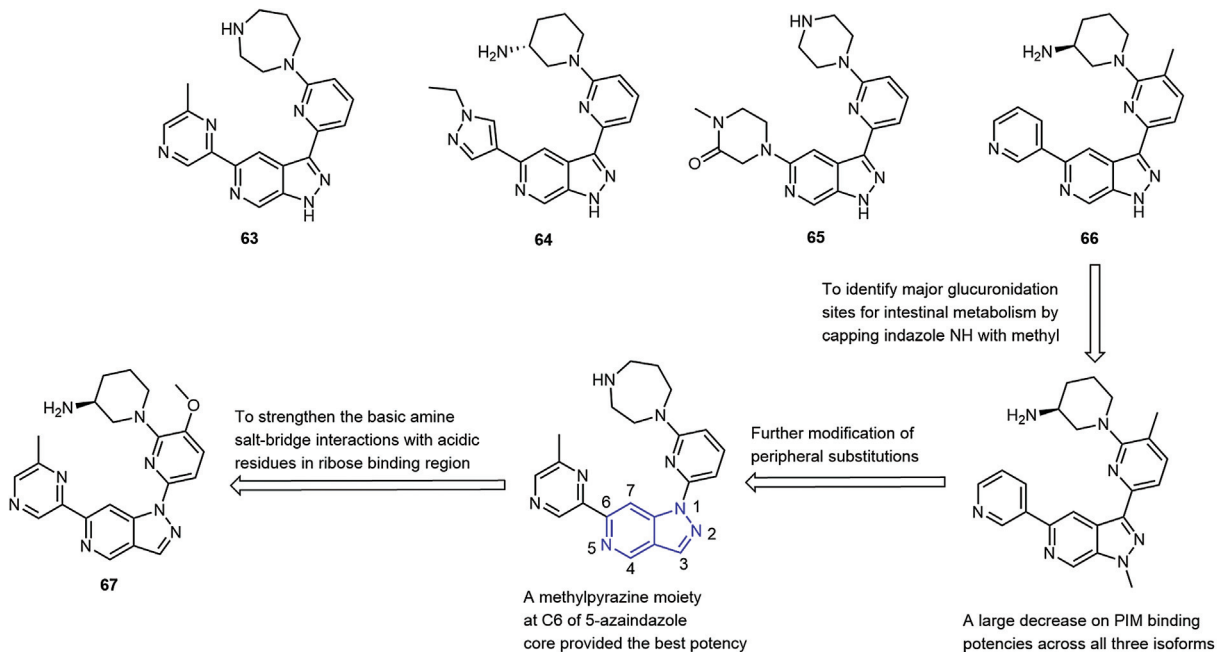


**Fig. 13** Representative compounds of 5-azaindazole derivatives.

Preliminary SAR showed that increasing the polarity of the substituent at 2-position could reduce hERG inhibitory activity and increase the solubility of the candidates; therefore, further optimization by Barberis et al led to the generation of **75**, which had the potential to suppress tumor growth in a KG1 tumor-bearing mouse model (► **Fig. 15**).<sup>69</sup>

In 2020, Barberis et al highlighted that attempts to increase target kinases' potencies only led to adverse drug properties and therefore focused on identifying compounds with desired indexes between cellular potency, ADME liabilities, and with ligand efficiency.<sup>70</sup> In this work, the most potent analog **76** demonstrated significant inhibitory activity with an EC<sub>50</sub> value of 61 nmol/L against KG1 cell



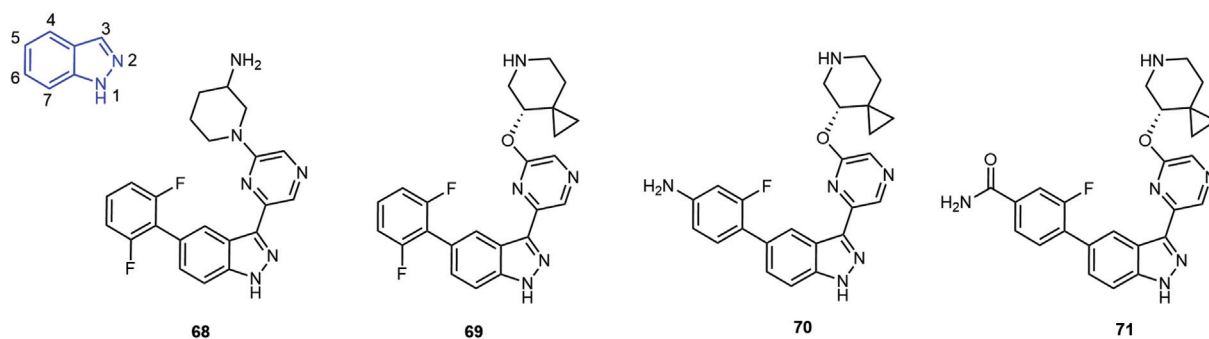


**Fig. 14** Representative compounds of 2-azaindazole derivatives.

lines, and oral administration of **76** at a dose of 150 mg/kg led to a tumor growth inhibition of 87% in a KG1 tumor xenograft model. Moreover, molecular docking study of **76** bound to PIM1 kinase (PDB code: 6VRV) was also illustrated. It was shown that compared with previous 2-position analogs, **76** showed good potency and increased ligand efficiency. Most gratifying, **76** had low affinity for the hERG ion channel, which was previously troublesome to overcome in this chemotype. When **76** was iv injected (3 mg/kg) and orally given (10 mg/kg) to rats, the short half-life of the compound was 2.7 hours due to high clearance (4.5 L/h/kg) and high volume of distribution (9.9 L/kg).

Nakano et al found **77** through HTS and its  $IC_{50}$  value of inhibiting PIM1 kinase was  $\sim 410$  nmol/L (**Fig. 15**).<sup>71</sup> The co-crystallization structure confirmed the formation of a hydrogen bond between the 3-carbonyl group of benzofuran and the 1-NH group of indole with Lys67 and Glu121, respectively, and the two aromatic rings formed hydrophobic interactions with the surrounding amino acids. **78** was further optimized to selectively inhibit PIM1 and Flt-3 with  $IC_{50}$  values of 6 and 47 nmol/L over 50 kinases. **78** effectively inhibited the growth of leukemia cell MV4-11 with a  $GI_{50}$  value of 43 nmol/L, but had no effect on normal human cells. In addition, **78** has good ADMET properties,

including good stability in human and mouse liver microsomes, no significant inhibitory effect on five major CYP450 kinases, and moderate hERG inhibitory activity.

Nakano et al identified that **79** has strong PIM1 inhibitory activity, but its kinase selectivity is not as good as **78** (**Fig. 15**).<sup>72</sup> They presumed that the nitrogen atom at 7-position of the indazole ring may interact with the amino acids in the hinge region of other kinases. With high water solubility, membrane permeability, and low hERG inhibitory activity, researchers expected to improve the kinase selectivity of **79** on the basis of retaining ADMET properties through structural modification. The introduction of a suitable 6-substituent in the 7-azaindole ring would be sterically tolerated by PIM and hydrogen bond between 7-position nitrogen of the 7-azaindole ring, and off-target kinases would be blocked, thereby the selectivity for PIM kinase increased. The chloro-substituted derivative **80** showed acceptable *in vitro* ADMET properties.

## Conclusion

PIM kinase is the key node of tumor cell signal transduction. It promotes the occurrence and development of tumor by regulating the process of cell cycle, accelerating transcription and translation, and inhibiting apoptosis. PIM kinase

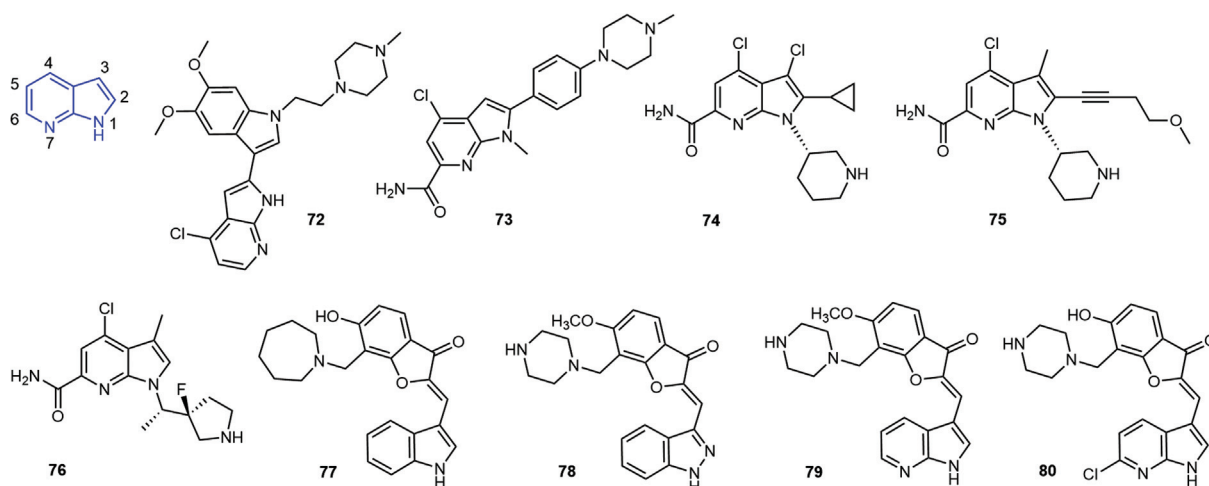


**Fig. 15** Representative compounds of 7-azaindazole derivatives.

inhibitors with high efficiency and low toxicity are therefore deemed necessary to become a new strategy for cancer and immunoregulation. This article reviewed the latest research progress of pan-PIM kinase inhibitors from different angles, summarizing molecule docking characteristics, PK properties as well as enzymatic and cell-based activities supported by structure-based design attributes. Although no highly selective PIM kinase inhibitor has been approved for now, several varieties have entered clinical trials. It is believed that this kind of small-molecule inhibitors will reignite new hope for patients in cancer therapy and immunomodulation with the continuous advance of research.

#### Funding

The work was approved by the Natural Science Foundation of Shanghai with Grant No. 19ZR1437900.

#### Conflict of Interest

None.

#### References

- Brault L, Gasser C, Bracher F, Huber K, Knapp S, Schwaller J. PIM serine/threonine kinases in the pathogenesis and therapy of hematologic malignancies and solid cancers. *Haematologica* 2010;95(06):1004–1015
- Daenthanasanmak A, Wu Y, Iamsawat S, et al. PIM-2 protein kinase negatively regulates T cell responses in transplantation and tumor immunity. *J Clin Invest* 2018;128(07):2787–2801
- Eerola SK, Kohvakka A, Tammela TLJ, Koskinen PJ, Latonen L, Visakorpi T. Expression and ERG regulation of PIM kinases in prostate cancer. *Cancer Med* 2021;10(10):3427–3436
- Kunder R, Velyunskiy M, Dunne SF, et al. Synergistic PIM kinase and proteasome inhibition as a therapeutic strategy for MYC-overexpressing triple-negative breast cancer. *Cell Chem Biol* 2022;29(03):358.e5–372.e5
- Nawijn MC, Alendar A, Berns A. For better or for worse: the role of Pim oncogenes in tumorigenesis. *Nat Rev Cancer* 2011;11(01):23–34
- Narlik-Grassow M, Blanco-Aparicio C, Carnero A. The PIM family of serine/threonine kinases in cancer. *Med Res Rev* 2014;34(01):136–159
- Warfel NA, Kraft AS. PIM kinase (and Akt) biology and signaling in tumors. *Pharmacol Ther* 2015;151:41–49
- Jackson LJ, Pheneger JA, Pheneger TJ, et al. The role of PIM kinases in human and mouse CD4+ T cell activation and inflammatory bowel disease. *Cell Immunol* 2012;272(02):200–213
- Wu J, Chu E, Kang Y. PIM kinases in multiple myeloma. *Cancers (Basel)* 2021;13(17):4304
- Chatterjee S, Chakraborty P, Daenthanasanmak A, et al. Targeting PIM kinase with PD1 inhibition improves immunotherapeutic antitumor T-cell response. *Clin Cancer Res* 2019;25(03):1036–1049
- Liu Z, Han M, Ding K, Fu R. The role of Pim kinase in immunomodulation. *Am J Cancer Res* 2020;10(12):4085–4097
- Jacobs MD, Black J, Futer O, et al. Pim-1 ligand-bound structures reveal the mechanism of serine/threonine kinase inhibition by LY294002. *J Biol Chem* 2005;280(14):13728–13734
- Zhao Y, Aziz AUR, Zhang H, Zhang Z, Li N, Liu B. A systematic review on active sites and functions of PIM-1 protein. *Hum Cell* 2022;35(02):427–440
- Drygin D, Haddach M, Pierre F, Ryckman DM. Potential use of selective and nonselective Pim kinase inhibitors for cancer therapy. *J Med Chem* 2012;55(19):8199–8208
- Pogacic V, Bullock AN, Fedorov O, et al. Structural analysis identifies imidazo[1,2-b]pyridazines as PIM kinase inhibitors with in vitro antileukemic activity. *Cancer Res* 2007;67(14):6916–6924
- Chen LS, Redkar S, Bearss D, Wierda WG, Gandhi V. Pim kinase inhibitor, SGI-1776, induces apoptosis in chronic lymphocytic leukemia cells. *Blood* 2009;114(19):4150–4157
- Paño T, González-Méndez L, San-Segundo L, et al. Protein translation inhibition is involved in the activity of the Pan-PIM kinase inhibitor PIM447 in combination with pomalidomide-dexamethasone in multiple myeloma. *Cancers (Basel)* 2020;12(10):2743
- Iida S, Sunami K, Minami H, et al. A phase I, dose-escalation study of oral PIM447 in Japanese patients with relapsed and/or refractory multiple myeloma. *Int J Hematol* 2021;113(06):797–806
- Raab MS, Thomas SK, Ocio EM, et al. The first-in-human study of the pan-PIM kinase inhibitor PIM447 in patients with relapsed and/or refractory multiple myeloma. *Leukemia* 2019;33(12):2924–2933
- Mazzacurati L, Collins RJ, Pandey G, et al. The pan-PIM inhibitor INCB053914 displays potent synergy in combination with ruxolitinib in models of MPN. *Blood Adv* 2019;3(22):3503–3514
- Tao ZF, Hasvold LA, Leverson JD, et al. Discovery of 3H-benzo[4,5]thieno[3,2-d]pyrimidin-4-ones as potent, highly selective, and orally bioavailable inhibitors of the human protooncogene proviral insertion site in moloney murine leukemia virus (PIM) kinases. *J Med Chem* 2009;52(21):6621–6636
- López-Ramos M, Prudent R, Moucadel V, et al. New potent dual inhibitors of CK2 and Pim kinases: discovery and structural insights. *FASEB J* 2010;24(09):3171–3185
- Tsuhako AL, Brown DS, Koltun ES, et al. The design, synthesis, and biological evaluation of PIM kinase inhibitors. *Bioorg Med Chem Lett* 2012;22(11):3732–3738
- Pierre F, Stefan E, Nédellec AS, et al. 7-(4H-1,2,4-Triazol-3-yl)benzo[c][2,6]naphthyridines: a novel class of Pim kinase inhibitors with potent cell antiproliferative activity. *Bioorg Med Chem Lett* 2011;21(22):6687–6692
- Pastor J, Oyarzabal J, Saluste G, et al. Hit to lead evaluation of 1,2,3-triazolo[4,5-b]pyridines as PIM kinase inhibitors. *Bioorg Med Chem Lett* 2012;22(04):1591–1597
- Blanco-Aparicio C, Collazo AM, Oyarzabal J, et al. Pim 1 kinase inhibitor ETP-45299 suppresses cellular proliferation and synergizes with PI3K inhibition. *Cancer Lett* 2011;300(02):145–153
- Martínez-González S, Rodríguez-Aristegui S, Gómez de la Oliva CA, et al. Discovery of novel triazolo[4,3-b]pyridazin-3-yl-quinoline derivatives as PIM inhibitors. *Eur J Med Chem* 2019;168:87–109
- Casuscelli F, Ardini E, Avanzi N, et al. Discovery and optimization of pyrrolo[1,2-a]pyrazinones leads to novel and selective inhibitors of PIM kinases. *Bioorg Med Chem* 2013;21(23):7364–7380
- Bullock AN, Russo S, Amos A, et al. Crystal structure of the PIM2 kinase in complex with an organoruthenium inhibitor. *PLoS One* 2009;4(10):e7112
- Xia Z, Knaak C, Ma J, et al. Synthesis and evaluation of novel inhibitors of Pim-1 and Pim-2 protein kinases. *J Med Chem* 2009;52(01):74–86
- Beharry Z, Zemskova M, Mahajan S, et al. Novel benzylidene-thiazolidine-2,4-diones inhibit Pim protein kinase activity and induce cell cycle arrest in leukemia and prostate cancer cells. *Mol Cancer Ther* 2009;8(06):1473–1483
- Hiasa M, Teramachi J, Oda A, et al. Pim-2 kinase is an important target of treatment for tumor progression and bone loss in myeloma. *Leukemia* 2015;29(01):207–217
- Fujii S, Nakamura S, Oda A, et al. Unique anti-myeloma activity by thiazolidine-2,4-dione compounds with Pim inhibiting activity. *Br J Haematol* 2018;180(02):246–258
- Dakin LA, Block MH, Chen H, et al. Discovery of novel benzylidene-1,3-thiazolidine-2,4-diones as potent and selective inhibitors of

- the PIM-1, PIM-2, and PIM-3 protein kinases. *Bioorg Med Chem Lett* 2012;22(14):4599–4604
- 35 Keeton EK, McEachern K, Dillman KS, et al. AZD1208, a potent and selective pan-Pim kinase inhibitor, demonstrates efficacy in preclinical models of acute myeloid leukemia. *Blood* 2014;123(06):905–913
  - 36 Cortes J, Tamura K, DeAngelo DJ, et al. Phase I studies of AZD1208, a proviral integration Moloney virus kinase inhibitor in solid and haematological cancers. *Br J Cancer* 2018;118(11):1425–1433
  - 37 Harada M, Benito J, Yamamoto S, et al. The novel combination of dual mTOR inhibitor AZD2014 and pan-PIM inhibitor AZD1208 inhibits growth in acute myeloid leukemia via HSF pathway suppression. *Oncotarget* 2015;6(35):37930–37947
  - 38 Flanders Y, Dumas S, Caserta J, et al. A versatile synthesis of novel pan-PIM kinase inhibitors with initial SAR study. *Tetrahedron Lett* 2015;56(23):3186–3190
  - 39 Bataille CJ, Brennan MB, Byrne S, et al. Thiazolidine derivatives as potent and selective inhibitors of the PIM kinase family. *Bioorg Med Chem* 2017;25(09):2657–2665
  - 40 Quevedo CE, Bataille CJ, Byrne S, et al. Aminothiazolones as potent, selective and cell active inhibitors of the PIM kinase family. *Bioorg Med Chem* 2020;28(22):115724
  - 41 Sawaguchi Y, Yamazaki R, Nishiyama Y, et al. Rational design of a potent Pan-Pim kinases inhibitor with a rhodanine-benzimidazole structure. *Anticancer Res* 2017;37(08):4051–4057
  - 42 Lee J, Park J, Hong VS. Synthesis and evaluation of 5-(3-(pyrazin-2-yl)benzylidene)thiazolidine-2,4-dione derivatives as pan-pim kinases inhibitors. *Chem Pharm Bull (Tokyo)* 2014;62(09):906–914
  - 43 Yun Y, Hong VS, Jeong S, Choo H, Kim S, Lee J. 2-Thioxothiazolidin-4-one analogs as Pan-PIM kinase inhibitors. *Chem Pharm Bull (Tokyo)* 2021;69(09):854–861
  - 44 Burger MT, Han W, Lan J, et al. Structure guided optimization, in vitro activity, and in vivo activity of Pan-PIM Kinase inhibitors. *ACS Med Chem Lett* 2013;4(12):1193–1197
  - 45 Garcia PD, Langowski JL, Wang Y, et al. Pan-PIM kinase inhibition provides a novel therapy for treating hematologic cancers. *Clin Cancer Res* 2014;20(07):1834–1845
  - 46 Burger MT, Nishiguchi G, Han W, et al. Identification of N-(4-((1R,3S,5S)-3-Amino-5-methylcyclohexyl)pyridin-3-yl)-6-(2,6-difluorophenyl)-5-fluoropicolinamide (PIM447), a potent and selective proviral insertion site of moloney murine leukemia (PIM) 1, 2, and 3 kinase inhibitor in clinical trials for hematological malignancies. *J Med Chem* 2015;58(21):8373–8386
  - 47 Nishiguchi GA, Burger MT, Han W, et al. Design, synthesis and structure activity relationship of potent pan-PIM kinase inhibitors derived from the pyridyl carboxamide scaffold. *Bioorg Med Chem Lett* 2016;26(09):2328–2332
  - 48 Koblish H, Li YL, Shin N, et al. Preclinical characterization of INCB053914, a novel pan-PIM kinase inhibitor, alone and in combination with anticancer agents, in models of hematologic malignancies. *PLoS One* 2018;13(06):e0199108
  - 49 Ishchenko A, Zhang L, Le Brazidec JY, et al. Structure-based design of low-nanomolar PIM kinase inhibitors. *Bioorg Med Chem Lett* 2015;25(03):474–480
  - 50 Wang X, Blackaby W, Allen V, et al. Optimization of Pan-Pim kinase activity and oral bioavailability leading to diaminopyrazole (GDC-0339) for the treatment of multiple myeloma. *J Med Chem* 2019;62(04):2140–2153
  - 51 Wang X, Magnuson S, Pastor R, et al. Discovery of novel pyrazolo [1,5-a]pyrimidines as potent pan-Pim inhibitors by structure- and property-based drug design. *Bioorg Med Chem Lett* 2013;23(11):3149–3153
  - 52 Dwyer MP, Keertikar K, Paruch K, et al. Discovery of pyrazolo[1,5-a]pyrimidine-based Pim inhibitors: a template-based approach. *Bioorg Med Chem Lett* 2013;23(22):6178–6182
  - 53 Arias-Gómez A, Godoy A, Portilla J. Functional pyrazolo[1,5-a]pyrimidines: current approaches in synthetic transformations and uses as an antitumor scaffold. *Molecules* 2021;26(09):2708
  - 54 Foulks JM, Carpenter KJ, Luo B, et al. A small-molecule inhibitor of PIM kinases as a potential treatment for urothelial carcinomas. *Neoplasia* 2014;16(05):403–412
  - 55 Nishiguchi GA, Atallah G, Bellamacina C, et al. Discovery of novel 3,5-disubstituted indole derivatives as potent inhibitors of Pim-1, Pim-2, and Pim-3 protein kinases. *Bioorg Med Chem Lett* 2011;21(21):6366–6369
  - 56 More KN, Jang HW, Hong VS, Lee J. Pim kinase inhibitory and antiproliferative activity of a novel series of meridianin C derivatives. *Bioorg Med Chem Lett* 2014;24(11):2424–2428
  - 57 More KN, Hong VS, Lee A, Park J, Kim S, Lee J. Discovery and evaluation of 3,5-disubstituted indole derivatives as Pim kinase inhibitors. *Bioorg Med Chem Lett* 2018;28(14):2513–2517
  - 58 Haddach M, Michaux J, Schwaebe MK, et al. Discovery of CX-6258. A potent, selective, and orally efficacious pan-Pim kinases inhibitor. *ACS Med Chem Lett* 2011;3(02):135–139
  - 59 Wang M, Tzintzun R, Gao M, Xu Z, Zheng QH. Synthesis of [<sup>11</sup>C] CX-6258 as a new PET tracer for imaging of Pim kinases in cancer. *Bioorg Med Chem Lett* 2015;25(18):3831–3835
  - 60 Rebello RJ, Kusnadi E, Cameron DP, et al. The dual inhibition of RNA Pol I transcription and PIM kinase as a new therapeutic approach to treat advanced prostate cancer. *Clin Cancer Res* 2016;22(22):5539–5552
  - 61 Zheng J, Sha Y, Roof L, et al. Pan-PIM kinase inhibitors enhance Lenalidomide's anti-myeloma activity via cereblon-IKZF1/3 cascade. *Cancer Lett* 2019;440–441:1–10
  - 62 Hu H, Wang X, Chan GK, et al. Discovery of 3,5-substituted 6-azaindazoles as potent pan-Pim inhibitors. *Bioorg Med Chem Lett* 2015;25(22):5258–5264
  - 63 Wang X, Kolesnikov A, Tay S, et al. Discovery of 5-azaindazole (GNE-955) as a potent Pan-Pim inhibitor with optimized bio-availability. *J Med Chem* 2017;60(10):4458–4473
  - 64 Wang HL, Cee VJ, Chavez F Jr, et al. The discovery of novel 3-(pyrazin-2-yl)-1H-indazoles as potent pan-Pim kinase inhibitors. *Bioorg Med Chem Lett* 2015;25(04):834–840
  - 65 Tandon N, Luxami V, Kant D, Tandon R, Paul K. Current progress, challenges and future prospects of indazoles as protein kinase inhibitors for the treatment of cancer. *RSC Adv* 2021;11(41):25228–25257
  - 66 Motati DR, Amaradhi R, Ganesh T. Azaindole therapeutic agents. *Bioorg Med Chem* 2020;28(24):115830
  - 67 Barberis C, Moorcroft N, Arendt C, et al. Discovery of N-substituted 7-azaindoles as PIM1 kinase inhibitors - Part I. *Bioorg Med Chem Lett* 2017;27(20):4730–4734
  - 68 Barberis C, Moorcroft N, Pribish J, et al. Discovery of N-substituted 7-azaindoles as Pan-PIM kinase inhibitors - Lead series identification - Part II. *Bioorg Med Chem Lett* 2017;27(20):4735–4740
  - 69 Barberis C, Pribish J, Tserlin E, et al. Discovery of N-substituted 7-azaindoles as Pan-PIM kinases inhibitors - Lead optimization - Part III. *Bioorg Med Chem Lett* 2019;29(03):491–495
  - 70 Barberis C, Erdman P, Czekaj M, et al. Discovery of SARxxxx92, a pan-PIM kinase inhibitor, efficacious in a KG1 tumor model. *Bioorg Med Chem Lett* 2020;30(23):127625
  - 71 Nakano H, Saito N, Parker L, et al. Rational evolution of a novel type of potent and selective proviral integration site in Moloney murine leukemia virus kinase 1 (PIM1) inhibitor from a screening-hit compound. *J Med Chem* 2012;55(11):5151–5164
  - 72 Nakano H, Hasegawa T, Kojima H, Okabe T, Nagano T. Design and synthesis of potent and selective PIM kinase inhibitors by targeting unique structure of ATP-binding pocket. *ACS Med Chem Lett* 2017;8(05):504–509